Journal of Physics: Theories and Applications E-ISSN: 2549-7324 / P-ISSN: 2549-7316
J. Phys.: Theor. Appl. Vol. 10 No. 1 (2026) 1-11 doi: 10.20961/jphystheor-appl.v10i1.108005

Improvement of microstructures and dielectric properties of coprecipitation iron (Fe)-doped barium titanate

Muazaroh Nur Azizah[1], Dianisa Khoirum Sandi[2], Khairuddin[1], Fahru Nurosyid[1], Trya Andini[1], and Yofentina Iriani[1]

[1]Department of Physics, Faculty of Mathematics and Natural Sciences, Universitas Sebelas Maret, Surakarta 57126, Indonesia
[2]Study Program of Energy Conversion Engineering, Department of Mechanical Engineering, Politeknik Negeri Semarang, Semarang 50275, Indonesia

Corresponding author's e-mail: yofent_iriani@staff.uns.ac.id

Received 13 August 2025, Revised 13 February 2026, Published 31 March 2026

Abstract: Barium titanate ($BaTiO_3$ or BTO) is a famous lead-free ferroelectric material often studied due to its fascinating features for technological applications. However, its performance requires continuous enhancement, one approach being doping with iron (Fe). This study aimed to demonstrate the improvement in the microstructures and dielectric properties of barium titanate induced by iron doping. The barium titanate and iron-doped barium titanate with the formula of $BaTi_{1-x}Fe_xO_3$ (x = 0, 0.01, 0.03, and 0.05) were synthesized using the coprecipitation technique. X-ray diffraction (XRD) analysis confirmed the formation of a pure tetragonal phase in all samples, while Fourier-transform infrared (FTIR) spectroscopy revealed characteristic BTO absorption bands at around 500 cm^{-1}. Compared with pure BTO, Fe-doped samples exhibited increased lattice constants, crystallite sizes, densities, and dielectric constants. Further, the dielectric constants of the samples were also higher than those of undoped barium titanate. These results indicate that Fe doping enhances the microstructures of BTO, leading to improved dielectric performance.

Keyword: barium titanate; coprecipitation; iron doping; dielectric constant; microstructure

1. Introduction

Significant lifestyle changes and the escalation of industrial and technological developments demand a high need for energy, especially electricity, which is driving much research on energy harvesting and storage. In particular, current energy storage devices that are widely used are capacitors. The advantages of capacitors compared to others, such as batteries, are that they possess high power density (~104 – 105 W/kg), fast charge-discharge rate, stable temperature/ frequency, and more durable performance against high temperatures and voltages (Adamczyk-Habrajska, Wodecka-Dus, Goryczka, & Makowska, 2024; Wodecka-Dus, Kozielski, Makowska, Bara, & Adamczyk-Habrajska, 2022; Zhang, Yao, Hao, Cao, & Liu, 2022). The simplest dielectric capacitor

structure consists of two metal plates arranged in parallel. These two plates are separated by a dielectric material or insulator, which will polarize when subjected to an electric field (Islam, Momin, & Nesa, 2019). A dielectric material is crucial in capacitors since it determines how much a capacitor can accommodate electrical charges, which is called capacitance.

Ferroelectrics are a type of material that is recognized for its characteristics of a high dielectric constant. Accompanied by their fundamental characteristic of having permanent dipole moments and spontaneous polarizations, ferroelectrics are extensively exploited for the manufacture of multilayer ceramic capacitors (MLCCs), ferroelectric random access memories (FRAMs), thermistors, and detectors (Alshoaibi, Kanoun, Ul Haq, AlFaify, & Goumri-Said, 2020; Li, Yu, Hao, & Janolin, 2022; More et al., 2021). One famous free-lead ferroelectric material often studied is barium titanate ($BaTiO_3$ or BTO) due to its fascinating features for technological applications. It has a perovskite ABO_3 structure where Ba^{2+} locates the A site created by the associated octahedral and Ti^{4+} ions occupy the B site with an octahedral cage (Nayak & Nayak, 2023; Noguchi & Matsuo, 2021). It also has a relatively low Curie temperature (120 ^oC for bulk) and is known for excellent dielectric, ferroelectric, and piezoelectric properties (Reda, El-Dek, & Arman, 2022; Sato, Haruta, Sasagawa, Ohta, & Jongprateep, 2019).

The performance of BTO needs to be continuously improved for its real-life applications. It can be improved by adjusting the microstructures through various treatments, including synthesis methods, sintering temperature and times, and doping. It is recognized that most of the chemical and physical properties of the material can be enhanced through the dopant ions. Understanding the influence of dopants on the electronic structure is a crucial step to improving the material's properties. Doping leads to modification in the ferroelectric properties, electrical properties, and dielectric properties of perovskite BTO, depending upon the dopant size substitution taking place either at the A or B site in the ABO_3 perovskite structure (Sato et al., 2019; Singh, Dixit, & Dobal, 2021a). Various types of dopants, such as Sr, Bi, Y, W, Co, Zr, etc., were incorporated to determine their effects on barium titanate properties (Alshoaibi et al., 2020; Iriani, Sandi, Kusumandari, & Sarifah, 2023; Iriani, Suherman, Sandi, Nurosyid, Khairuddin, et al., 2024; Kumar, Thakur, & Luthra, 2018; Mukherjee, Ghosh, Ghosh, & Mitra, 2013; Nayak & Nayak, 2023; Reda et al., 2022). Among them, iron dopants are preferred as Fe^{3+} has a radius of 0.645 Å, close to that of Ti^{4+} of 0.605 Å.

Particularly, BTO is conventionally synthesized using the familiar solid-state reaction method (Kumar et al., 2018; Veerapandiyan et al., 2019; Zhou et al., 2020). However, the technique produces a material with high porosity and large particle size, which is unbeneficial for the electronic properties of BTO (Iriani, Kusumandari, Ulfa, & Sandi, 2022; Iriani et al., 2023). Besides, this method is usually performed at a high sintering temperature and extended time, consuming energy (Khirade, Birajdar, Raut, & Jadhav, 2016; Xiong, Xiao, Yao, Liu, & Hao, 2024). To overcome this matter, wet chemical procedures can be employed since they can yield materials with fine and homogeneous particle sizes (Iriani et al., 2022; Iriani et al., 2023; Iriani, Suherman, Sandi, Nurosyid, Khairuddin, et al., 2024). Additionally, these procedures are conducted at low

temperatures and in a relatively short time. Several wet chemical methods have been used to synthesize barium titanate, including chemical coprecipitation, hydrothermal, sol-gel, etc (Mukherjee et al., 2013; Singh et al., 2021a; Suherman, Nurosyid, Khairuddin, Sandi, & Irian, 2022). The coprecipitation method is chosen because it is relatively straightforward and has low operational costs.

The influences of doping on the fundamental and electronic properties of BTO have been studied by preparing BTO primarily through solid-state and chemical techniques. Still, reports on the synthesis of iron-doped nanocrystalline BTO through the coprecipitation technique have scarcely been discovered. Therefore, this study was conducted to fabricate iron-doped BTO ($BaTi_{1-x}Fe_xO_3$) nanocrystalline using the coprecipitation technique and further investigate the influences of iron dopant concentrations on the microstructures and dielectric properties of the prepared materials.

2. Method

The synthesis of iron-doped BTO with the formula of $BaTi_{1-x}Fe_xO_3$ (x = 0, 0.01, 0.03, and 0.05) was done using the coprecipitation technique. The starting materials were barium hydroxide ($Ba(OH)_2$) [Sigma Aldrich, 95%], titanium tetrabutoxide ($Ti(C_4H_9O)_4$) [Sigma Aldrich, 97%], Oxalic acid dihydrate ($C_2H_2O_4.2H_2O$) [Sigma Aldrich ≥ 99%], Isopropanol (IPA), ferric nitrate nonahydrate ($Fe(NO_3)_3.9H_2O$) [Sigma Aldrich ≥ 99%], ethanol, polyvinyl alcohol (PVA).

First, the oxalic acid dihydrate was dissolved in the IPA solution by stirring for 20 min (Sol 1). Then, titanium tetrabutoxide was separately diluted into the IPA solution by stirring for 20 min (Sol 2). Sol 1 and Sol were mixed, barium hydroxide and ferric nitrate nonahydrate were added to the mixture, and stirred for 30 min. The final solution was then added with distilled water, stirred for 1 hour, and kept for 24 hours. Afterward, it was filtered to obtain the precipitate and then washed with ethanol and distilled water until pH 6 was obtained. This precipitate was hydrolyzed at 100 °C for 5 hours to achieve dried samples. The dried samples were then crushed and pressed using a hydraulic press (100 MPa) to get the pellet samples. Finally, they were sintered at 1000 °C for 4 hours. The samples were later called BT, BTF1, BTF3, and BTF5 for undoped barium titanate, $BaTi_{0.99}Fe_{0.01}O_3$, $BaTi_{0.97}Fe_{0.03}O_3$, and $BaTi_{0.95}Fe_{0.05}O_3$, respectively. The prepared samples were characterized using X-ray diffraction (XRD) (Bruker D8 Advanced with Cu source Kα of 1.5406 Å), Fourier Transform Infrared Spectroscopy (FTIR) (Shimadzu A21004802518), and RLC meters (GW Instek LCR meter 7819) to determine their crystal structure, functional groups, and dielectric properties.

3. Results and Discussion

Figure 1 denotes the XRD patterns of barium titanate doped with various iron concentrations. The patterns matched with the PCPDF data No. 831880, validating the formation of tetragonal perovskite of BTO. The inset of Figure 1 presents the influence of iron doping on the XRD characteristic peaks, revealing a right shift in the (101) peaks. This indicates that the doping has been successfully performed. Further, it denotes that crystal structure parameters have been modified. Nevertheless, the marks (* and +) in the

patterns exhibit the existence of trash in the prepared materials. These trashes were confirmed as $BaCO_3$ (PCPDF no 410373) and BaC_2O_4 (PCPDF no 190125), emerging because the raw materials were incompletely reacted during the synthesis process. This might be due to the Ba^{2+} ions in the solution, which react rapidly with carbon dioxide in the environment (Padchasri et al., 2021).

Table 1 presents the lattice constant, crystallite size (D), and tetragonality (c/a) of the prepared samples. Both using the Scherer and William-Hall plot methods, the crystallite sizes of iron-doped barium titanate were larger than those of undoped barium titanate. This means that iron doping may stimulate crystal growth during the sintering process. Still, the crystallite size enlarged linearly at iron doping at x from 0 to 0.03. At x = 0.05, it turned to decrease, which might be due to excessive dopant concentration. The lattice constants of iron-doped barium titanate also tended to increase than that of undoped barium titanate. The tetragonality values of the samples were also varied between undoped and doped barium titanate.

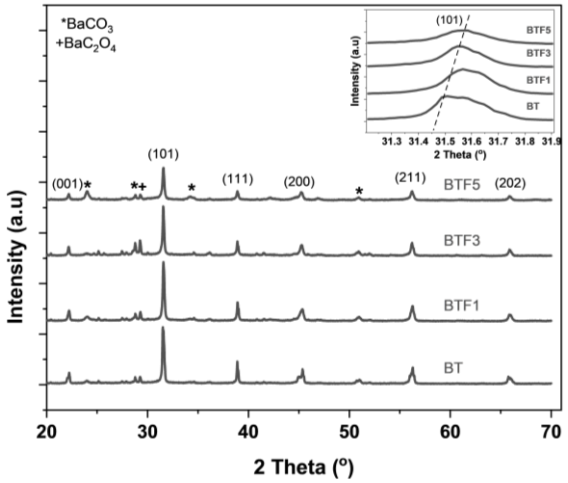

Figure 1. XRD patterns of pure and iron-doped barium titanate samples

Table 1. Crystal structure parameters of the prepared samples

Samples	D (nm)	D (nm)	Lattice Constant		Tetragonality
	Scherrer	WH plot	*a*=*b*(Å)	*c*(Å)	*c*/*a*(Å)
BT	38.3	35.4	4.0042	4.0038	0.9999
BFT1	42.2	38.6	4.0029	4.0014	0.9996
BFT3	46.7	42.4	4.0045	4.0056	1.0002
BFT5	41.4	32.7	4.0088	4.0045	0.9989

Figure 2 displays the FTIR spectra of the undoped and doped barium titanate in the wavenumbers of 400 – 4000 cm^{-1}. No significant changes were detected in the peak positions as iron doping was given. The considerable peaks at about 544 – 561 cm^{-1} corresponded to the Ti-O bonds, corresponding to the formation of BTO (More et al., 2021; Tihtih, Limame, Ababou, Sayouri, & Ibrahim, 2019). The peak shift in the Ti-O bonds due to the iron doping denotes the change in the unit cell size, in this case, the lattice constant (Arijun, Mahabub, Mohammad, & Shamima, 2020; Tihtih et al., 2019).

The peaks at around 856 – 558 cm^{-1} were related to the TiO_6 vibrations. The peaks at about 1425 – 1442 cm^{-1} denoted the presence of the carbonyl groups associated with the trash in the samples (More et al., 2021; Tihtih et al., 2019). Meanwhile, the peaks at 3447 – 3456 cm^{-1} were correlated to the hydroxyl groups due to weakly bound water interaction with its environment via hydrogen bonding (Khirade et al., 2016; Yulianingsih & Munasir, 2016).

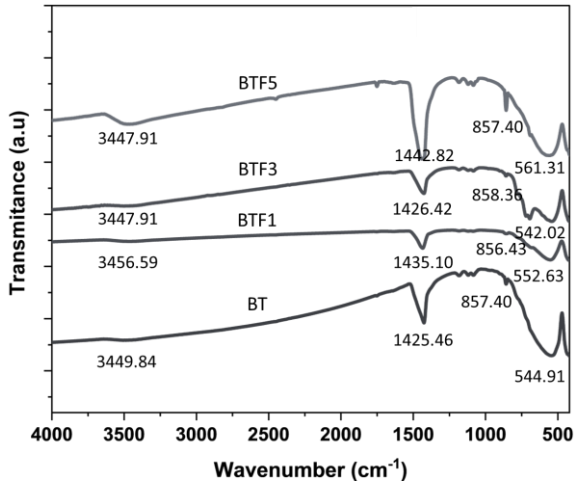

Figure 2. FTIR spectra of undoped and doped barium titanate

Table 2. Measured, theoretical, and relative densities and porosities of the undoped and doped barium titanate

Sample	Measured density (g/cm^3)	Theoretical density (g/cm^3)	Relative density (%)	Porosity (%)
BT	4.0692	6.0194	67.6011	32.3989
BFT1	4.6653	6.0411	77.2265	22.7735
BFT3	5.1654	6.0331	85.6174	14.3826
BFT5	4.1820	6.0403	69.2357	30.7643

Table 2 exhibits the theoretical, measured, and relative density values of the undoped and doped barium titanate. The theoretical density of the samples in this study was in the range of 6.0194 to 6.0411g/cm^3, which is close to the standard theoretical density of barium titanate in the literature (DeChiara, Momjian, Wang, & Randall, 2024; Sufiiarov, Kantyukov, Popovich, & Sotov, 2021). Further, it shows that iron doping has increased the measured and relative density of the samples, meaning a reduction in porosity. It demonstrates that iron doping helps to promote the densification of the material (Kumar et al., 2018; Reda et al., 2022). It reveals that the density linearly improved from x=0 (undoped) to iron doping (x=0.03), then it decreased at iron doping (x=0.05).

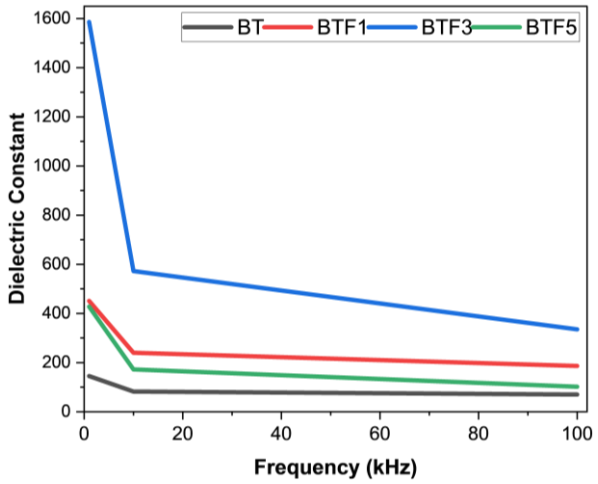

Figure 3. Frequency-dependence of dielectric constant

The testing using the LCR meter produced capacitance data that can be converted into dielectric constant through the formula of $K = Cd/A\varepsilon_o$. In which K, C, d, A, and ε_o are the dielectric constant, capacitance, pellet thickness, pellet area, and vacuum dielectric permittivity (8.85 x 10^{-12} Farad/m), respectively (Fan, Long, & Hu, 2021; Tang et al., 2024). Figure 3 exhibits the relation between frequency and dielectric constant. It is a normal phenomenon that the dielectric constant decreases at high frequencies due to the influence of the polarization by the applied field (Rajan, Gazzali, & Chandrasekaran, 2017; Singh, Dixit, & Dobal, 2021b; Wang & Yang, 2023). At low frequencies, the dipoles in a dielectric material have time to respond to changes in the electric field, so the dielectric constant tends to be higher. Meanwhile, as the electric field frequency increases, the dipoles cannot keep up with the changes as quickly, causing the dielectric constant to decrease. At very high frequencies, the dielectric constant tends to reflect only the response of the electrons in the material (Fan et al., 2021; Rayssi, El Kossi, Dhahri, & Khirouni, 2018; Wang & Yang, 2023).

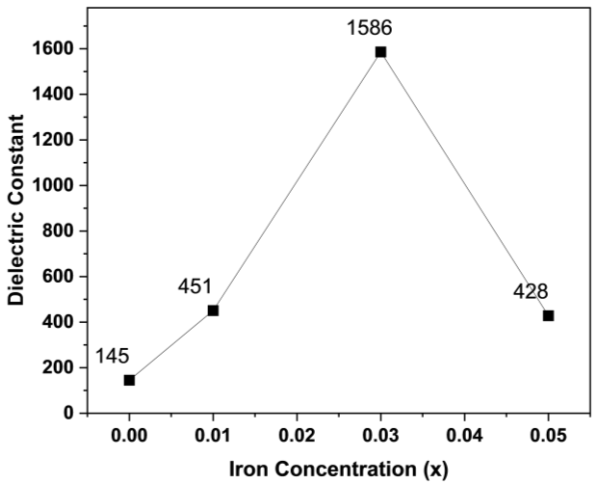

Figure 4. Dielectric constant as a function of iron concentrations at 1 kHz

Figure 4 presents the dielectric constant of the samples as a function of iron doping concentration. It demonstrates that the dielectric constants improved linearly from x = 0

to x = 0.03; then, they declined at an excessive iron doping of x=0.05. This trend is the same as the results in the crystallite size and density of the samples. Nevertheless, all iron-doped samples exhibited higher dielectric constants than pure BTO. Several aspects, including density, porosity, crystallite sizes, tetragonality, frequency, etc, can influence the dielectric constant (Iriani, Suherman, Sandi, Nurosyid, & Handoko, 2024; Kumar et al., 2018; Wang & Yang, 2023). Further, the maximum values of the dielectric constant for BTF5 composition could be attributed to its highest density due to the impact of iron doping. A denser material provides more space for dipoles to move freely, increasing the dielectric constant (Kumar et al., 2018; Zechao Li, 2022).

Overall, the yields revealed that the dielectric properties of barium titanate improved due to Fe doping. The study by Singh et al. (Singh et al., 2021b) exhibited distinct results that the dielectric constants reduced with the incorporation of Fe and increasingly declined with increasing Fe content. Singh et al. synthesized Fe-doped barium titanate via the sol-gel method, while this study employed the coprecipitation method that induced distinct structural properties affecting the dielectric constants. If compared, the synthesis using the coprecipitation in this study could produce a larger crystal size with the addition of Fe, which has a role in providing a free movement of dipoles, thereby improving the dielectric properties. Another similar study by Boyar et al. (Bhoyar et al., 2020) also revealed that the dielectric constants of Fe-doped barium strontium titanate prepared by the sol-gel method declined with higher Fe doping, which might be due to the decreased grain size. This finding suggests that this study demonstrated a better result of Fe doping on the properties of barium titanate.

Furthermore, this study has implications. Fe doping into the barium titanate structure can modify its dielectric properties, potentially improving this material's performance in applications such as capacitors and piezoelectric devices. Nevertheless, this study has several limitations. First, the coprecipitation method requires exact control of pH, temperature, and reagent concentration to ensure homogeneous Fe doping in the BTO matrix. Minor parameter variations can lead to compositional inhomogeneities, negatively impacting material properties. Second, Fe doping can lead to the formation of unwanted secondary phases (Figure 1) that can affect the dielectric properties and stability of the material. Third, although the coprecipitation method is effective at the laboratory scale, its application at the industrial scale may face challenges related to reproducibility and consistency of product quality.

For improvement, further research can be focused on optimizing the synthesis parameters, such as pH, temperature, and reaction time, to achieve more homogeneous Fe doping and reduce the formation of secondary phases. Furthermore, the use of advanced characterization techniques, such as impedance spectroscopy and high-resolution electron microscopy, can provide a deeper understanding of the relationship between the microstructure and the dielectric properties of the material. Third, exploring the effects of doping with other elements or multiple doping combinations can open up opportunities to further improve the material properties according to specific application needs. Finally, exploring other synthesis methods, such as hydrothermal, can help

overcome the limitations of the coprecipitation method and improve the quality and consistency of the resulting materials.

Lastly, this research has the potential to significantly impact various fields of physics, especially materials physics and technological applications. This research can enrich the understanding of how transition metal doping, such as Fe, affects the ferroelectric and dielectric properties of $BaTiO_3$. This is relevant for studying phase transitions and spontaneous polarization phenomena in ferroelectric materials. Next, Fe doping can modify the electronic structure of BTO, affecting the material's band gap, which is essential in the design of photocatalytic devices and sensors based on ferroelectric materials. Further, BTO is a key ingredient in multilayer capacitors. The enhancement of dielectric properties through Fe doping can produce capacitors with higher capacitance and better temperature stability. Moreover, materials with high and stable dielectric properties are suitable for applications in solid-state batteries and energy storage devices based on supercapacitors.

4. Conclusion

The pure and Fe-doped $BaTiO_3$ with various Fe concentrations have been successfully synthesized with the coprecipitation technique. The formation of the pure tetragonal phase of undoped and doped nanocrystalline barium titanate has been confirmed with the XRD data. The iron doping has enlarged the crystallite sizes of the samples. Besides, the iron doping enhanced the density of the samples and reduced their porosity. Further, the increase in these microstructures led to an improved dielectric constant. The optimum dielectric constant was achieved by the sample with an iron doping concentration of $x = 0.03$ due to its highest density. Still, iron-doped barium titanate samples demonstrated enhanced microstructure properties, thereby improving the dielectric constant. Further research may focus on varying the doping of other elements or multi-doping combinations to strengthen stability and dielectric properties.

Acknowledgements

The authors thank the 2024 Research Group Grant by Universitas Sebelas Maret, with contract no 194.2/UN27.22/PT.01.03/2024, for funding this research.

References

Adamczyk-Habrajska, M., Wodecka-Dus, B., Goryczka, T., & Makowska, J. (2024). Impedance Spectroscopy of Fe and La-Doped $BaTiO_3$ Ceramics. *Crystals, 14*(2), 131. doi:10.3390/cryst14020131

Alshoaibi, A., Kanoun, M. B., Ul Haq, B., AlFaify, S., & Goumri-Said, S. (2020). Insights into the Impact of Yttrium Doping at the Ba and Ti Sites of $BaTiO_{(3)}$ on the Electronic Structures and Optical Properties: A First-Principles Study. *ACS Omega, 5*(25), 15502-15509. doi:10.1021/acsomega.0c01638

Arijun, N., Mahabub, A. B., Mohammad, J. R., & Shamima, C. (2020). Enhanced Dielectric properties of Bismuth Doped Barium Titanate Ceramics with their Structural and Compositional Studies. *Biointerface Research in Applied Chemistry, 11*(3), 9862-9870. doi:10.33263/briac113.98629870

Bhoyar, D. N., Somvanshi, S. B., Nalle, P. B., Mande, V. K., Pandit, A. A., & Jadhav, K. M. (2020). Multiferroic Fe^{3+} ion doped $BaTiO_3$ Perovskite Nanoceramics: Structural, Optical, Electrical and Dielectric Investigations. *Journal of Physics: Conference Series, 1644*(1), 012058. doi:10.1088/1742-6596/1644/1/012058

DeChiara, J. A., Momjian, S., Wang, K., & Randall, C. A. (2024). Bimodal grain sized barium titanate dielectrics enabled under the cold sintering process. *Open Ceramics, 19*, 100626. doi:10.1016/j.oceram.2024.100626

Fan, J., Long, Z., & Hu, Z. (2021). High dielectric performance and multifarious polarizations in (Lu + Ta) co-doped TiO_2 ceramics. *Journal of Asian Ceramic Societies, 9*(3), 1255-1264. doi:10.1080/21870764.2021.1966919

Iriani, Y., Kusumandari, Ulfa, U., & Sandi, D. K. (2022). Synthesis of $BaTiO_3$ Ceramics Using Coprecipitation and Solid-State Reaction Method with Sintering Temperature Variation. *Materials Science Forum, 1064*, 89-97. doi:10.4028/p-de85ci

Iriani, Y., Sandi, D. K., Kusumandari, & Sarifah, N. (2023). Investigation of Barium Strontium Titanate ($Ba_{0.95}Sr_{0.05}TiO_3$) synthesized via conventional solid-state reaction and coprecipitation route with diverse sintering temperatures. *Materials Today: Proceedings*. doi:10.1016/j.matpr.2023.02.229

Iriani, Y., Suherman, B., Sandi, D. K., Nurosyid, F., & Handoko, E. (2024). Microstructure, Atomic Bonds, and Dielectric Characteristics of Neodymium (Nd)-doped Barium Titanate. *Evergreen, 11*(3), 2063-2070. doi:10.5109/7236851

Iriani, Y., Suherman, B., Sandi, D. K., Nurosyid, F., Khairuddin, Handoko, E., & Faquelle, D. (2024). Structural Modification and Dielectric Property of Bi-Doped $BaTiO_3$ ($Ba_{1-x}Bi_xTiO_3$) Ceramics with coprecipitation Technique. *Integrated Ferroelectrics, 240*(1), 140-148. doi:10.1080/10584587.2023.2296318

Islam, M. A., Momin, M. A., & Nesa, M. (2019). Effect of Fe doping on the structural, optical and electronic properties of $BaTiO_3$: DFT based calculation. *Chinese Journal of Physics, 60*, 731-738. doi:10.1016/j.cjph.2019.06.013

Khirade, P. P., Birajdar, S. D., Raut, A. V., & Jadhav, K. M. (2016). Multiferroic iron doped $BaTiO_3$ nanoceramics synthesized by sol-gel auto combustion: Influence of iron on physical properties. *Ceramics International, 42*(10), 12441-12451. doi:10.1016/j.ceramint.2016.05.021

Kumar, S., Thakur, O. P., & Luthra, V. (2018). Modulating the Effect of Yttrium Doping on the Structural and Dielectric Properties of Barium Titanate. *physica status solidi (a), 215*(7), 1700710. doi:10.1002/pssa.201700710

Li, Z., Yu, J., Hao, S., & Janolin, P.-E. (2022). Enhancing properties of lead-free ferroelectric $BaTiO_3$ through doping. *Journal of the European Ceramic Society, 42*(12), 4693-4701. doi:10.1016/j.jeurceramsoc.2022.05.023

More, S., Khedkar, M. V., Kulkarni, G. D., Kadhane, P., Kamble, R., & Jadhav, K. M. (2021). Effect of iron doping on structural, DC electrical resistivity and ferroelectric properties of $BaTiO_3$ nanoceramics. *Optik, 247*, 167913. doi:10.1016/j.ijleo.2021.167913

Mukherjee, S., Ghosh, S., Ghosh, C., & Mitra, M. K. (2013). Synthesis and Characterization of Iron Doped Nano Barium Titanate Through Mechanochemical Route. *Journal of The Institution of Engineers (India): Series D, 94*(1), 57-64. doi:10.1007/s40033-013-0019-z

Nayak, P., & Nayak, S. K. (2023). Doping effect of Fe, Co and W on the structural, electrical and magnetic properties of $BaTiO_3$ ferroelectric ceramics. *Solid State Communications, 371*, 115272. doi:10.1016/j.ssc.2023.115272

Noguchi, Y., & Matsuo, H. (2021). Ferroelectric photovoltaic tensor in visible-light-active Fe-doped BaTiO3single crystals. *Japanese Journal of Applied Physics, 60*(SF), SFFA01. doi:10.35848/1347-4065/ac0c6c

Padchasri, J., Triamnak, N., Sareein, T., Jutimoosik, J., Tongsaeng, S., Bootchanont, A., . . . Yimnirun, R. (2021). Crystal structure and XANES study of Fe-substituted Barium Titanate ceramics prepared by conventional solid-state technique. *Radiation Physics and Chemistry, 188*, 109657. doi:10.1016/j.radphyschem.2021.109657

Rajan, S., Gazzali, P. M. M., & Chandrasekaran, G. (2017). Impact of Fe on structural modification and room temperature magnetic ordering in $BaTiO_{(3)}$. *Spectrochim Acta A Mol Biomol Spectrosc, 171*, 80-89. doi:10.1016/j.saa.2016.07.037

Rayssi, C., El Kossi, S., Dhahri, J., & Khirouni, K. (2018). Frequency and temperature-dependence of dielectric permittivity and electric modulus studies of the solid solution Ca(0.85)Er(0.1)Ti(1-x) Co(4x/3)O(3) (0 </= x </= 0.1). *RSC Adv, 8*(31), 17139-17150. doi:10.1039/c8ra00794b

Reda, M., El-Dek, S. I., & Arman, M. M. (2022). Improvement of ferroelectric properties via Zr doping in barium titanate nanoparticles. *Journal of Materials Science: Materials in Electronics, 33*(21), 16753-16776. doi:10.1007/s10854-022-08541-x

Sato, N., Haruta, M., Sasagawa, K., Ohta, J., & Jongprateep, O. (2019). Fe and Co-doped (Ba, Ca)TiO_3 Perovskite as Potential Electrocatalysts for Glutamate Sensing. *Engineering Journal, 23*(6), 265-278. doi:10.4186/ej.2019.23.6.265

Singh, D., Dixit, A., & Dobal, P. S. (2021a). Effect of Structural Changes on the Electrical Properties of Sol-gel derived Iron Doped Barium Titanate. *Journal of Physics: Conference Series, 2070*(1), 012054. doi:10.1088/1742-6596/2070/1/012054

Singh, D., Dixit, A., & Dobal, P. S. (2021b). Effect of Structural Changes on the Electrical Properties of Sol-gel derived Iron Doped Barium Titanate. *Journal of Physics: Conference Series, 2070*(1). doi:10.1088/1742-6596/2070/1/012054

Sufiiarov, V., Kantyukov, A., Popovich, A., & Sotov, A. (2021). Structure and Properties of Barium Titanate Lead-Free Piezoceramic Manufactured by Binder Jetting Process. *Materials, 14*(16), 4419. doi:10.3390/ma14164419

Suherman, B., Nurosyid, F., Khairuddin, Sandi, D. K., & Irian, Y. (2022). Impacts of low sintering temperature on microstructure, atomic bonds, and dielectric constant of barium titanate ($BaTiO_3$) prepared by coprecipitation technique. *Journal of Physics: Conference Series, 2190*(1), 012006. doi:10.1088/1742-6596/2190/1/012006

Tang, Q., Shi, Z., Xia, S., Bie, X., Yang, Y., Bian, D., . . . Fan, R. (2024). Enhanced dielectric properties of Sr^{2+} and Zr^{4+} doped $BaTiO_3$ colossal permittivity metamaterials. *EPJ Applied Metamaterials, 11*, 13. doi:10.1051/epjam/2024012

Tihtih, M., Limame, K., Ababou, Y., Sayouri, S., & Ibrahim, J.-E. F. M. (2019). Sol-gel synthesis and structural characterization of Fe doped barium titanate nanoceramics. *Epitoanyag - Journal of Silicate Based and Composite Materials, 71*(6), 190-193. doi:10.14382/epitoanyag-jsbcm.2019.33

Veerapandiyan, V. K., Deluca, M., Misture, S. T., Schulze, W. A., Pilgrim, S. M., & Tidrow, S. C. (2019). Dielectric and structural studies of ferroelectric phase evolution in dipole-pair substituted barium titanate ceramics. *Journal of the American Ceramic Society, 103*(1), 287-296. doi:10.1111/jace.16713

Wang, H., & Yang, L. (2023). Dielectric constant, dielectric loss, conductivity, capacitance and model analysis of electronic electroactive polymers. *Polymer Testing, 120*, 107965. doi:10.1016/j.polymertesting.2023.107965

Wodecka-Dus, B., Kozielski, L., Makowska, J., Bara, M., & Adamczyk-Habrajska, M. (2022). Fe-Doped Barium Lanthanum Titanate as a Competitor to Other Lead-Free Piezoelectric Ceramics. *Materials (Basel), 15*(3), 1089. doi:10.3390/ma15031089

Xiong, P., Xiao, M., Yao, Z., Liu, H., & Hao, H. (2024). Improving the Energy Storage Performance of Barium Titanate-Based Ceramics through the Addition of ZnO-Bi_2O_3-SiO_2 Glass. *Crystals, 14*(3). doi:10.3390/cryst14030242

Yulianingsih, A., & Munasir. (2016). Analisis Komposit Fe3O4/c-SiO2 dari Pasir Talaud Lumajang. *Jurnal Inovasi Fisika Indonesia, 5*(2), 5-8.

Zechao Li, J. Y., Shenglan Hao, Pierre-Eymeric Janolin. (2022). Enhancing properties of lead-free ferroelectric $BaTiO_3$ through doping. *Journal of the European Ceramic Society,, 42*(12), 4693-4701. doi:10.1016/j.jeurceramsoc.2022.05.023

Zhang, N., Yao, Z., Hao, H., Cao, M., & Liu, H. (2022). Selectively designed Fe doping of lead-free $BaTiO_3$ piezoceramics. *Journal of Materials Science: Materials in Electronics, 33*(13), 10154-10164. doi:10.1007/s10854-022-08005-2

Zhou, L., Zhang, Y., Li, S., Lian, Q., Yang, J., Bai, W., & Tang, X. (2020). Fe doping effect on the structural, ferroelectric and magnetic properties of polycrystalline $BaTi_{1-x}Fe_xO_3$ ceramics. *Journal of Materials Science: Materials in Electronics, 31*(17), 14487-14493. doi:10.1007/s10854-020-04008-z